Premixed Methane/Air/Hydrogen Flame Oscillations in Horizontal Open End Tubes

Houshi Jiang, Amaludin N.A, Woolley, R and Yang Zhang.
Department of Mechanical Engineering, University of Sheffield
Sheffield, S1 3JD, United Kingdom

1 Introduction

Flammable hydrocarbon gases are widely utilized, however, during production, transportation, storage and utilization they have the potential to mix with air, ignite and detonate [1],[2]. Following ignition of a premixture the flame initially propagates as a deflagration but following interaction with the environment it can accelerate leading to a denotation (known as Deflagration to Detonation Transition (DDT)). One of the earliest studies of premixed flame propagation was that of Mallard and Le Chatelier who ignited flames in tubes to examine the problem of coal mining explosion accidents [3]. They demonstrated that significant alterations in the flame propagation rate occurred as the flame travelled down the tube [3]. Other researches went on to study flame propagation in tubes in order to understand the mechanism of flame movements [4-7]. The flame vibration has been attributed to induced pressure oscillations which if in phase can satisfy Rayleigh's criteria [8] resulting in enhanced burn rates.

In combustion light emissions from the excited species formed during chemical reactions are known as flame chemiluminescence. Flame chemiluminescence measurements have received increasing attention from researchers as they can provide useful information on the combustion process in conjunction with high speed imaging. Huang and Zhang explored C_2^* chemiluminescence intensities utilizing RGB colour channels [9]. Subsequently Yang et al. applied this method to flame propagation in tube, demonstrating the impact of pressure fluctuations [10]. The work reported here is an extension of previous studies, flame propagation down a tube was monitored using simultaneous C_2^* chemiluminescence and pressure measurements. In this study, a ϕ =1.2 methane-hydrogen-air (R_H 0.2) flames have been filmed propagating within a 1200 mm long horizontal tube of 20 mm internal diameter quartz tube open at both ends.

2 Experimental Setup

The system is based around a 1200 mm long horizontal tube of 20 mm internal diameter with both ends open to atmosphere. The ambient temperature of the lab was approximately 293 K. Following each experiment the tube was evacuated using a vacuum pump. The required volume of fuel was injected into the apparatus using a syringe and air introduced into the rig to bring it to atmospheric pressure. R_H is a

Correspondence to: yz100@sheffield.ac.uk

parameter defining the amount of hydrogen concentration in a fuel mixture, first implemented by Yu et al. [11]. The measurements reported here were performed with methane-hydrogen-air mixtures (R_H 0.2) at equivalence ratio 1.2. This mixture was chosen following the work of Ebieto et al. [12], which found that the mixture produced highly oscillating flames. The experiment was repeated 20 times and result is representative of those runs. The mixture was ignited using a pilot flame placed at one end of the tube. The quartz tube provided optical access allowing the flame propagation to be recorded. A Photron SA-4 high speed colour camera with a Nikon 35-200 mm, f-3.5 zoom lens, a framing rate of 1000 fps and 1000 μs shutter speed was used to record the flame position. Pressure measurements were also collected using a Kistler Type 7261 piezo-electric pressure transducer mounted at end of the tube furthest from the ignition point. The camera and pressure transducer were synchronized.

Colour images were processed by using a Matlab code to provide C_2^* emission levels based on the characterisation of the colour signal emanating from the flame. The combustion radical C_2^* was calculated from the blue and green channel values in the camera's RGB colour space, it showed good correlation with the C_2^* chemiluminescence intensities, verified and explained in detail by Huang and Zhang [9].

3 Results and Analysis

Figure 1 shows the calculated total intensity of C_2^* and the pressure signal at the end of the tube. The propagation of the flame was categorized in four stages. Each stage of propagation is associated with different flame shapes which are displayed in Figure 2:

Stage 1: During the first stage the intensity of C_2^* increased slightly but there was no change in pressure which remained at its pre-ignition value. The flame propagated convex to the direction of travel. The convex or flame finger shape is due to the non-slip condition at the wall acting on the burnt gasses as well as heat transfer from the reaction zone to the wall [11]. Its shape was not symmetrical with a tail at the bottom of the tube, this has been attributed to the effect of buoyancy forces on the flame. It may just be an artefact of ignition method as non-symmetrical flames have been observed in downwardly propagating flames [13].

Stage 2. The intensity of C_2^* dropped, corresponding to the flattening of the flame. Oscillations can be observed in both the pressure and C_2^*. The maximum amplitude of the pressure oscillation increased with each cycle.

Stage 3. Here the C_2^* and pressure signals achieved their maximum amplitudes. Reduction in flame speed accompanied by a pressure build-up initiates the third stage of the propagation, a parametric oscillating flame. In the first two frames, a long tail forms in the middle of the burned mixture which may be due to pressure gradient acting from the unburned to burned mixture resulting in a Rayleigh-Taylor instability [13] or Tulip flame. Following the creation of the tail the flame front collapses and becomes almost spherical ball (see image at 765 ms).

Stage 4 Here the C_2^* emission remained relatively constant whilst the pressure levels decayed down to were again achieved in stage 4, similar to stage 1.

Shown in Figure 3 are flame position and pressure histories. The flame position can be referenced by finding the leading and trailing edges. During stage 1, the flame propagated at ~2.5 m/s (approximately 5 times the laminar burning velocity) as shown. In stage 2, both the flame and pressure starts to pulsate, and the flame flattens, deaccelerates the speed to ~1.8 m/s. The peak pressure reached values of 130 Pa. Flame size reduction in stage 2 leads to a decrease in C_2^*. At its maximum point, the pressure achieves 895 Pa and the flame attains a maximum propagation speed of 4.5 m/s. Performing a Fast Fourier Transform on both the distance amplitude and C_2^* signals revealed that the oscillatory components have frequencies of ~ 245 Hz. The pressure starts to decay beyond this point, and the shortening of the tulip flame length, ultimately slowing the front of the flame to -0.17 m/s although the back of the flame continues to propagate

forward. The intensity of C_2^* reduces at this point, the flame speed then increases back to the initial propagation speed of ~2.5 m/s and the pressure within the tube stops oscillating.

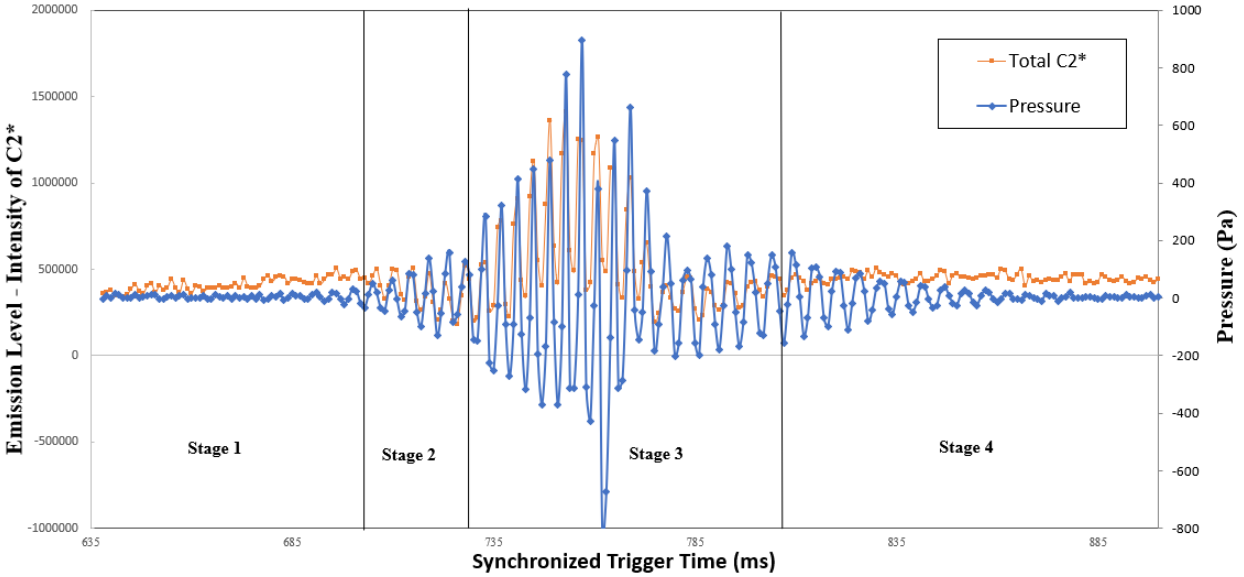

Figure 1. Calculated total intensity of C_2^* and pressure during the flame propagation.

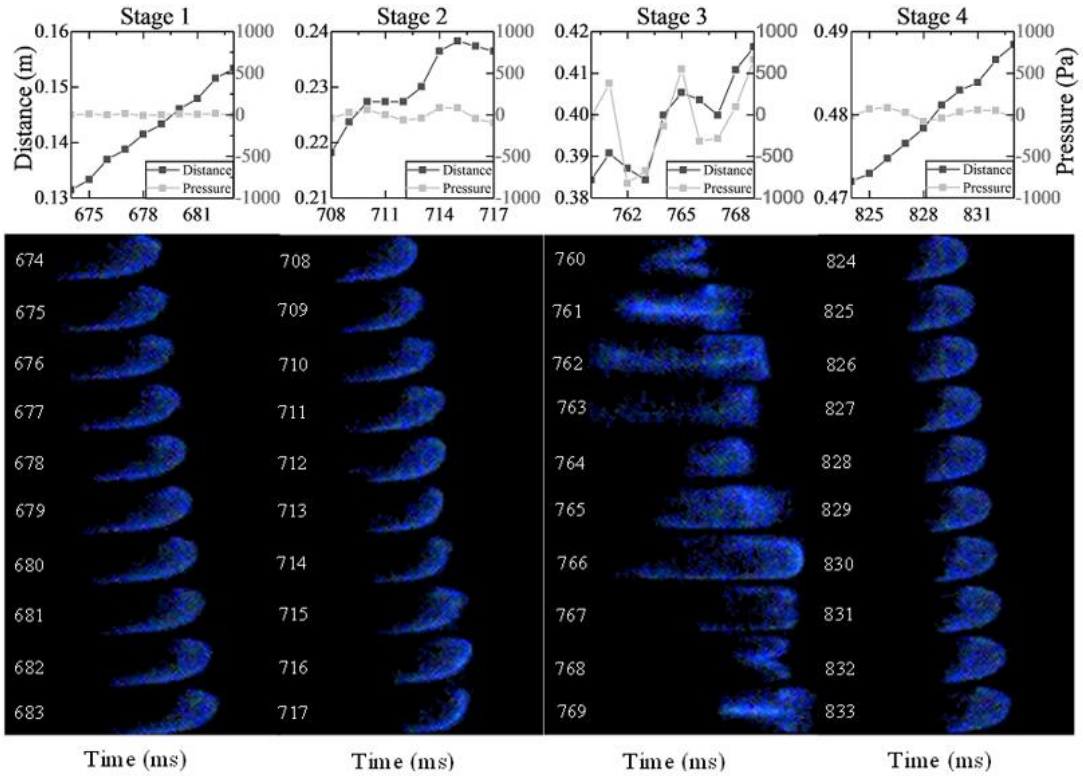

Figure 2. Sample image sequence of all stages with their respective time, pressure and distance. The unburnt black area of all images were cropped for clarity. The RGB channel values were selectively enhanced by multiplying the identified flame pixel 30 times for presentation.

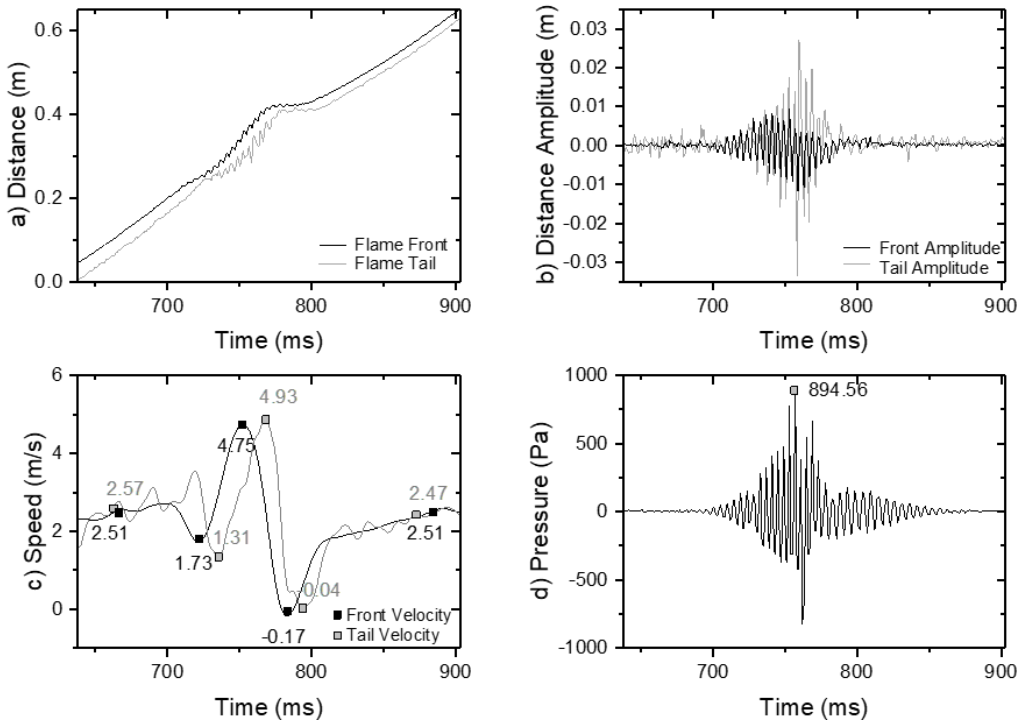

Figure 3: (a) distance of flame front (b) distance amplitude (c) flame speed calculate based on flame front position (d) pressure data

A variety of behaviours are displayed by the flame as it passes through the self-generated pressure field. The position and frequency of the oscillation are artefacts of the tube. If a different tube length was used, they would change, however, if a different mixture was ignited, they would stay broadly the same [14]. The magnitude of the pressure and resulting movement of the gas column are the consequence of the interaction between the pressure fluctuations, and the flame. To further investigate the interaction, the phase difference between the pressure signals and the flame was determined. The existence of a similar oscillatory frequency in the flame front, tail, C2* and pressure show the existence of a coupling interaction. A Hilbert Transform was applied to the time signals to extract their phase information. Prior to performing Hilbert Transform, the oscillatory components need to be isolated from the wideband frequency that exists within the time signals to remove the contribution from other frequency bands [15].

A 20th order finite impulse response band pass filter (cut-off frequency 100 Hz and 300 Hz) was used to isolate the ~245 Hz oscillation observed in the time signals. A Hilbert transform was then performed and the phase information for the flame front, tail, C2* intensity and pressure were obtained. The pressure phase was used as the reference, producing 3 plots of phase difference, pressure-front, pressure-tail and pressure-C2* intensity, shown in Figure 4 respectively. The fluctuating phase in Figure 4(a) and 4(c) represented the different stages discussed previously quite well. The coupling in stages 2 and 3 were confirmed by the minimal phase fluctuation at ~ 0°, while stage 1 and 4 were decoupled, indicated by the high phase difference fluctuation. However, the coupling in stage 2 and 3 cannot be observed in Figure 4(b), indicating that the flame tail does not couple with the pressure fluctuations.

Plots of phase difference against pressure amplitude, shown in Figure 4(d), 4(e) and 4(f) were plotted to observe the impact of phase difference on the pressure amplitude as used by, for example Kim et. al (16) and Coats et. al (17). It can be seen in Figures 4(d) and 4(f) that whenever the phase difference falls within

90 °(in-phase), the pressure amplitude starts to amplify, and dampens whenever it is beyond 90 ° (out of phase). From Figure 4(e) shows that the flame tail does not couple with the acoustic field.

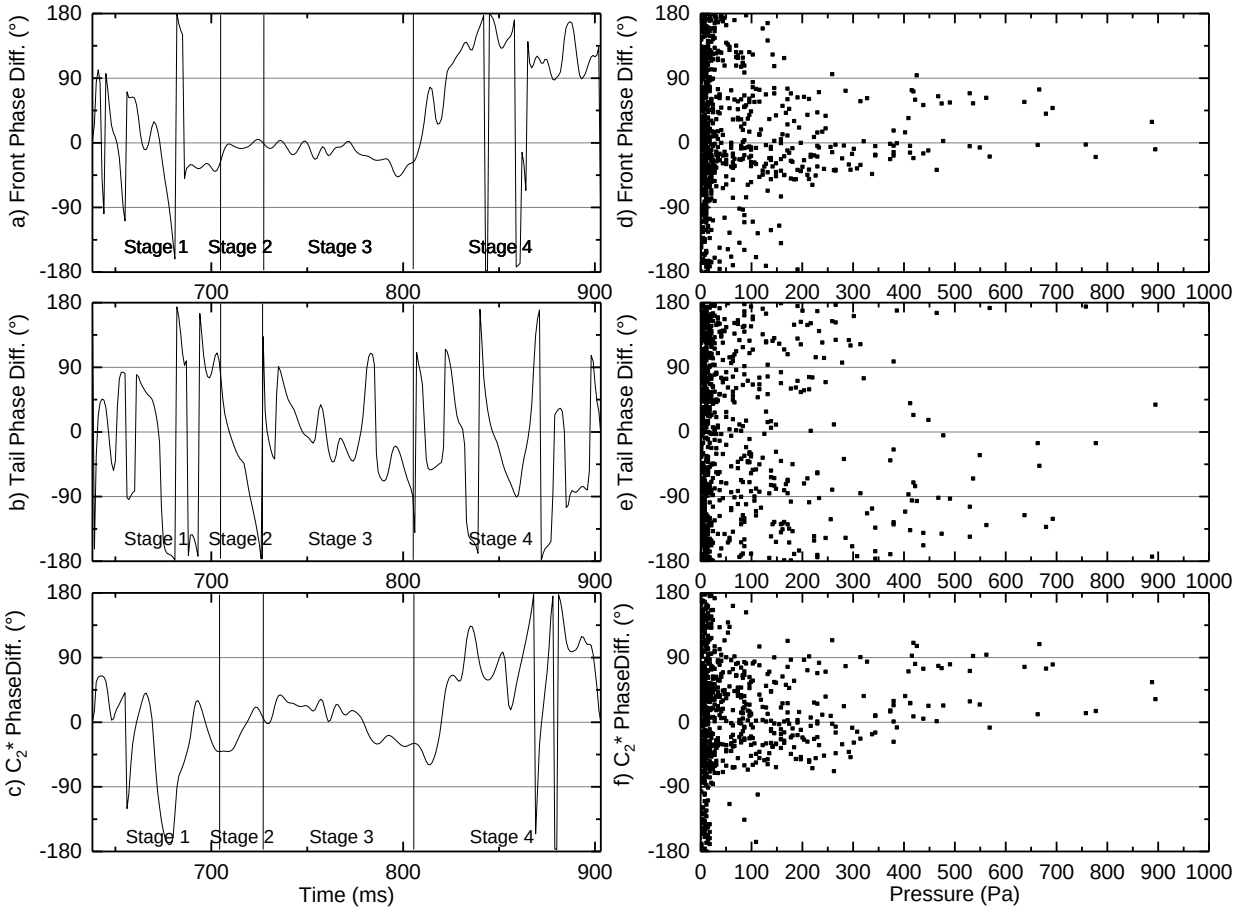

Figure 4: Flame-pressure phase difference: (a) flame front b) flame tail, and c) flame C_2* intensity. Compilation of flame pressure phase difference against pressure amplitude, (d) flame front e) flame tail, and f) flame C_2* intensity.

As the flame enters the acoustic field it falls into phase with the pressure fluctuations. As the flame progresses and the pressure amplitude increases there was a significate impact on the flame shape. Whilst the flame front position and C_2* intensity (which depends on the flame area) fluctuate in phase with the pressure oscillations, the rear of the flame does not. The action of the pressure waves to push spikes of unburned mixture into a burned gas this mixture can take time to burn up and is not impacted by the pressure wake induced fluctuations. This is likely to be the cause of some of spikes in peak pressure observed in Figure 3(b) resulting in unexpected large pressures.

4.Conclusion

A study was conducted to determine the relationship between the C_2^* chemiluminescence and the pressure oscillations using a 20 mm internal diameter, 1200 mm long tube, with both ends open. A quartz tube was used to provide optical access for high-speed colour imaging and a pressure transducer for collecting the pressure signal at the end of the tube. Main conclusions of the study are:

1. Four stages were identified: curved flame, flattened flame, parametric flame (maximum oscillation), and normalizing flame.
2. The measured C_2^* emissions have similar fluctuations with the measured pressure as the flame traverses down the tube. The results present the coupling interaction between flame chemiluminescence and pressure. The two signals are in phase in stage 2. The C_2^* and pressure reached maximum oscillation in stage 3.
3. The fluctuations in flame front position and C_2^* were found to vary in phase with the pressure fluctuations. The observed flame position at the rear of the flame was not in-phase with the pressure although the complex flame shapes that were observed were caused be the pressure and flow oscillations. This is thought to result in some of the observed sudden jumps in the peak pressure.

5. References

[1] Bjerketvedt, D., Bakke, J. R., and Van Wingerden, K. (1997). Gas Explosion Handbook. vol. 52, no. 96, pp. 1–150.
[2] Dorofeev, S. B. (2011). Flame acceleration and explosion safety applications. Proc. Combust. Inst., vol. 33, no. 2, pp. 2161–2175.
[3] Mallard E. F., Le Chatelier H. (1883). Combustion of explosive gas mixtures. Ann Mine.
[4] Wheeler, R.V. (1914). CCXLIII. The propagation of flame in mixtures of methane and air. The "uniform movement.". Journal of the Chemical Society, Transactions 105: 2606-2613
[5] Coward, H.F., Hartwell, F.J. (1932). Studies in the mechanism of flame movement. Part I. The uniform movement of flame in mixtures of methane and air, in relation to tube diameter. Journal of the Chemical Society (Resumed): 1996-2004.
[6] Gerstein, M, Levine, O, Wong, E.L. (1951). Flame propagation. II. The determination of fundamental burning velocities of hydrocarbons by a revised tube method. Journal of the American Chemical Society. 73: 418-422.
[7] Markstein, G. H. (1964). Nonsteady flame propagation, Ed. G.H. Markstein. Pergamon Press, New York.
[8] Rayleigh, J. W. S. (1896). The Theory of Sound: Volume 1, Dover Publications. New York.
[9] Huang, H.W. and Zhang, Y. (2008). Flame colour characterization in the visible and infrared spectrum using a digital camera and image processing. Meas. Sci. Technol. vol. 19, no. 8, p. 085406.
[10] Yang, J., Mossa, F.M.S., Huang, H.W., Wang, Q., Woolley, R., and Zhang, Y. (2015). Oscillating flames in open tubes. Proc. Combust. Inst. vol. 35, no. 2, pp. 2075–2082.
[11] Yu, G., Law, C.K., Wu. (1986). Laminar Flame Speeds of Hydrocarbon + Air Mixtures with Hydrogen Addition. Combustion and Flame. 63: 339-347.
[12] Ebieto, C. E., Amaludin, N.A., Woolley, R. (2015). Methane/Hydrogen/Air Flame Oscillations in Open Ended Tubes. 25th ICDERS.
[13] Ebieto, C.E. (2017). Dynamics of Premixed Flames in Tube, University of Sheffield.
[14] Clanet, C., Searby, G. (1996). On the "Tulip Flame" Phenomenon. Combustion and Flame. 105: 225-238.
[15] Cohen M. X. (2014). Analyzing Neural Time Series Data, MIT Press, Massachusetts.
[16] Kim, K., Lee, J., Quay B.D., Santavicca D.A. (2011). The dynamic response of turbulent dihedral V flames: An amplification mechanism of swirling flames. Combustion and Flame. 183: 163-179.
[17] Coats, C.M, Chang, Z, Williams, P.D. (2010). Excitation of thermoacoustic oscillations by small premixed flames. Combustion and Flame. 157: 1037-1051.